Araştırma Makalesi
Adıyaman Üniversitesi
Mühendislik Bilimleri Dergisi
24 (2024) 502-515

CAM SANAYI ATIĞININ ÜÇLÜ ALKALI AKTIVATÖR SISTEMIYLE ÜRETILEN CÜRUF ESASLI GEOPOLIMER KOMPOZITLERIN FIZIKSEL, MEKANIK VE DURABILITE ÖZELLIKLERINE ETKISI

Mahfuz PEKGÖZ[1*], **İlker TEKİN** [2]

[1, 2]Karabük Üniversitesi, Mühendislik Fakültesi, İnşaat Mühendisliği Bölümü, Karabük, 78000, Türkiye

Geliş Tarihi/Received Date: 23.04.2024 Kabul Tarihi/Accepted Date:13.12.2024 DOI:10.54365/adyumbd.1590079

ÖZET

Demir-çelik endüstrisi ve cam sanayisinden elde edilen atıkların çevresel etkilerinin azaltılması amacıyla yapılan bu çalışmada, cam sanayi atığının üçlü alkali aktivatör sistemiyle üretilen çüruf esaslı geopolimer kompozitlerin fiziksel, mekanik ve durabilite özelliklerine etkisi incelenmiştir. Bu kapsamda, cam sanayi atığı olan silis tozu, belirli oranlarda öğütülmüş yüksek fırın cürufu yerine ikame edilmiştir. Üçlü alkali aktivatör olarak; 10M NaOH, $Na_2SiO_{3(aq)}$ çözeltisi ve Na_2SO_4 içerikli atık sinter külü kullanılmıştır. Deneysel çalışmada üretilen geopolimer kompozitlerin yayılma, su emme, büzülme, kapiler su emme, basınç dayanımı ve asit direnci deneyleri yapılmıştır. %5 oranında silis tozu ikame edilmesi, geopolimer kompozitlerin fiziksel, mekanik ve durabilite özelliklerini belirgin bir şekilde iyileştirdiğini göstermektedir. Silis tozu, kompozitlerin işlenebilirliğini %40-45 oranında artırmış; ayrıca büzülme, kapiler su emme katsayısı ve poroziteyi azaltarak asidik ortamlara karşı dayanıklılığı artırmıştır. Bu bulgular, endüstriyel atıkların geopolimer malzemelerde etkin bir şekilde kullanılarak çevresel etkilerinin minimize edilebileceği ve sürdürülebilir, ekonomik açıdan verimli malzemelerin üretilebileceği yönünde önemli bir potansiyel sunmaktadır.

Anahtar Kelimeler: *Cüruf, Sinter Külü, Silis Tozu, Fiziksel ve Mekanik özellikler, Asit Direnci*

EFFECT OF GLASS INDUSTRY WASTE ON THE PHYSICAL, MECHANICAL, AND DURABILITY PROPERTIES OF SLAG-BASED GEOPOLYMER COMPOSITES PRODUCED WITH A TERNARY ALKALI ACTIVATOR SYSTEM

ABSTRACT

This study, aimed at reducing the environmental impact of industrial waste from the steel and glass industries, investigates the effect of glass industry waste on the physical, mechanical and durability properties of slag-based geopolymer composites produced with a ternary alkali activator system. Silica powder, a waste product from the glass industry, was substituted for ground blastfurnace slag in specific proportions. The ternary alkali activator system used consists of 10M NaOH, Na_2SiO_3(aq) solution and sinter ash containing Na_2SO_4. Experimental tests were carried out on the produced geopolymer composites, including spread, water absorption, shrinkage, capillary water absorption, compressive strength and acid resistance. The substitution of 5% silica powder significantly improved the physical, mechanical and durability properties of the geopolymer composites. Silica powder increased the workability of the composites by 40-45% and reduced shrinkage, capillary water absorption and porosity while improving resistance to acidic media. These results represent a significant potential for the effective use of industrial waste in geopolymer materials, helping to minimise environmental impact and produce sustainable, economically efficient materials.

Keywords: *Slag, Sinter Ash, Silica Powder, Physical and Mechanical Properties, Acid Resistance*

---

*e-posta[1] : mahfuzpekgoz@karabuk.edu.tr ORCID ID: https://orcid.org/ 0000-0002-9529-8537 (Sorumlu Yazar)
e-posta[2] : ilkertekin@karabuk.edu.tr ORCID ID: https://orcid.org/ 0000-0001-7400-4790

1. Introduction

The glass industry is a crucial component of modern construction and technology sectors. However, its production processes generate waste that presents significant environmental and economic challenges. Among these wastes, silica powder (SP) is notable for its high SiO_2 content and is typically disposed of through waste management methods [1-2]. However, these disposal methods contribute to environmental issues and lead to the waste of an economically valuable resource [3]. In recent years, there has been increasing research into alternative uses for waste SP. Its high reactivity and fine particulate structure make it a valuable additive in the production of geopolymers [4-5]. Geopolymers, with their low carbon emissions and sustainability benefits, offer an environmentally friendly alternative to traditional binders. Their properties also make them an ideal matrix for waste recovery [6-7]. Studies have shown that the incorporation of SP into geopolymers positively affects mechanical strength, chemical resistance, and microstructural development [8-9]. Notable improvements in acid resistance and strength properties have been observed in SP-based geopolymers [10]. Furthermore, these applications contribute to achieving sustainable waste management goals by facilitating the recovery of glass industry waste [11-12].

The iron and steel industry generates substantial amounts of waste through various processes. Among these, steel slag (SS) and ground granulated blast furnace slag (GGBFS) are particularly notable due to their significant environmental and economic implications. SS contains high concentrations of calcium oxide (CaO), iron oxides (Fe_2O_3), and other oxide components, whereas GGBFS primarily comprises silica (SiO_2), alumina (Al_2O_3), and CaO. Both materials are highly compatible with alkaline activation, making them suitable binders in geopolymer systems and supporting the production of sustainable construction materials. Additionally, China is the world's largest steel producer, producing 137 million tonnes of stainless steel in 2022. However, the utilisation rate is less than 30%, which is significantly lower than in developed countries such as Japan, the United States and the United Kingdom, where the utilisation rate reaches 70% [13]. In Turkey alone, the cumulative amount of SS discarded has reached 5.5 million tonnes, with less than 30% of SS used in low value-added applications such as aggregates in asphalt mixes [14-15], fillers in foundation construction, cementitious additives in concrete and other applications [16-18]. GGBFS, a granulated by-product of iron ore reduction, features an amorphous structure that makes it an effective binder in geopolymer matrices. Its inclusion improves the mechanical strength of geopolymer systems while enhancing their resistance to acidic environments. Research indicates that geopolymers incorporating these materials demonstrate enhanced physical and mechanical properties, including improved water absorption, compressive strength, and shrinkage behavior [19-21]. Studies on the application of SS and GGBFS in geopolymer systems emphasize their considerable potential for both sustainability and performance improvement. SS, owing to its free CaO and MgO content, enhances the curing and hardening properties of geopolymers. Meanwhile, GGBFS contributes to superior physico-mechanical characteristics, such as lower water absorption rates and higher strength values [22]. Further investigations are needed to assess the potential incorporation of sinter ash (SA) wastes into geopolymer systems. This study highlights the novel use of waste SA containing 82% Na_2SO_4 as an activator, alongside traditional NaOH and Na_2SiO_3 activators, addressing a gap in the current literature. Sodium sulfate and sodium carbonate, naturally occurring compounds, effectively enhance the reaction mechanisms in slag-based systems [23-24]. The activation process of slag with Na_2SO_4 involves the dissolution of SiO_4 and AlO_4 units in the slag, facilitated by Na^+ and SO_4^{2-} ions, which actively participate in hydration reactions [25]. The primary hydration products identified in Na_2SO_4-activated slag systems are C-S-H gel and ettringite, contributing to the material's strength and stability [26].

The use of geopolymers presents notable challenges concerning shrinkage and acid resistance, which are vital for their long-term performance in a variety of applications. Shrinkage, which occurs during both the curing and drying stages, is frequently attributable to the densification and hardening of the polymeric network, which results in a reduction in volume. Such shrinkage can have a detrimental impact on the material's dimensional stability, leading to the formation of cracks and a subsequent compromise in the structural integrity of the geopolymer. Recent studies have emphasised the significance of regulating the mixture design, curing procedures and the incorporation of additives, such as fibres or chemical agents, to minimise shrinkage and enhance the durability of geopolymers [27]. With regard to acid resistance, geopolymers display greater resilience to acidic environments than traditional cement-based materials, due to the strong aluminosilicate network they possess. Nevertheless, prolonged exposure to highly corrosive acids, particularly at elevated temperatures or in concentrated solutions, can still result in degradation of geopolymers. The extent of this degradation is contingent upon a number of factors, including the specific raw materials employed, the curing conditions, and the structural characteristics of the geopolymer [28]. To enhance acid resistance, recent studies have concentrated on optimising geopolymer composition and incorporating supplementary materials, such as industrial by-products, which can augment their durability in harsh chemical environments [29].

In this study, SP, a glass industry waste with a chemical composition of 95% SiO_2, was used to compensate for the effects of free CaO present in SS and to improve the physical, mechanical and durability properties of GCs. SP was substituted for GGBFS at weight ratios of 5%, 10%, 15%, 20% and 25% to reduce costs and increase waste recycling. The performance of the GCs was evaluated through tests measuring workability (flowability), water absorption, shrinkage, capillary water absorption, compressive strength and acid resistance.

2. Materials and Methods

In this study, a variety of materials were used to prepare geopolymer composites (GCs), including ground granulated blast furnace slag (GGBFS), steel slag (SS), sinter ash (SA), and silica powder (SP). The GGBFS is a by-product of the iron manufacturing process and is employed as a binder in geopolymer production due to its pozzolanic properties, which contribute significantly to the strength and durability of the GCs. The SS (sieved <1 mm), a by-product of steelmaking, was incorporated with the objective of enhancing the mechanical properties of the GCs. This incorporation provides additional calcium and iron components that improve the material's overall stability. Subsequently, the SP was incorporated into the mixture to augment the silica content, thereby facilitating the formation of the aluminosilicate gel that endows the GCs with their distinctive chemical and mechanical properties. These materials were selected for their complementary roles in optimising the performance of the GCs, with detailed specifications provided in the following sections. The overall mixture design is depicted in Figure 1. Figure 2 shows the particle size distributions of the raw components, determined using a Laser Particle Sizer.

Figure 1. Images of a) GGBFS, b) SS, c) SA and d) SP

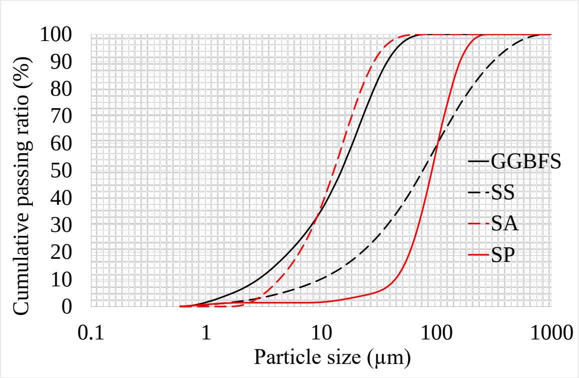

Figure 2. GGFS, SA, SS and SP particle size distributions used in study

The particle size distributions of GGBFS, SS and SA were analysed and showed different characteristics. GGBFS had D_{90}, D_{50} and D_{10} values of 37.5 µm, 14.9 µm and 2.52 µm respectively. In comparison, SS had much coarser D_{90}, D_{50} and D_{10} values of 309 µm, 76.1 µm and 9.84 µm. The SA showed intermediate particle sizes with D_{90}, D_{50} and D_{10} values of 32.6 µm, 14.6 µm and 4.89 µm. The SP showed intermediate particle sizes with D_{90}, D_{50} and D_{10} values of 161 µm, 91 µm and 43.5 µm. SS, after sieving to exclude particles larger than 1 mm, showed a particle size distribution primarily concentrated between 18 µm and 300 µm, as shown in Figure 2. In terms of specific surface area, GGBFS had a value of 403.4 m^2/kg, SS had 308.4 m^2/kg, SP had 173.7 m^2/kg and SA had the highest value of 576.1 m^2/kg. The respective densities of these materials were 2.98 kg/m^3 for GGBFS, 2.38 kg/m^3 for SS, 2.71 kg/m^3 for SP and 2.97 kg/m^3 for SA. Table 1 gives a detailed comparison of the chemical compositions of SS and GGBFS. It is noteworthy that SS has a higher free CaO content than GGBFS, which would suggest a higher reactivity. However, the higher Fe_2O_3 content in SS reduces its overall reactivity, distinguishing it from the finer and more active GGBFS.

Table 1. Chemical composition of SS and GGBFS

Oxides (%)	CaO	SiO_2	Al_2O_3	Fe_2O_3	MgO	SO_3	K_2O	Na_2O	Mn_2O_3	LOI
SS	48.01	12.82	2.58	13.9	3.19	2.09	0.04	-	3.48	13.31
GGBFS	30.13	36.01	11.49	1.65	8.66	0.63	0.84	0.60	5.66	-

In this study, high-purity NaOH (99.9%) at a concentration of 10 M and an aqueous sodium silicate solution (Na_2SiO_3) with a silica modulus (Ms) of 0.5 were utilized as activators in combination with SA. The 10M NaOH solution was selected based on the indication in the literature that the optimal mechanical and physical properties of geopolymers are typically observed with NaOH concentrations ranging from 10M to 14M [30]. The $Na_2SiO_{3(aq)}$ consisted of 12% Na_2O, 24% SiO_2, and 64% water. Additionally, waste by-products from the MEROS® process, carried out at the Karabük Iron and Steel Factory, were employed as an activator and surfactant in slag-based GCs. The MEROS® system in the iron and steel industry uses sodium bicarbonate to capture and solidify sulphates at elevated temperatures, producing a by-product known as SA. Kardemir Iron and Steel Factory generates approximately 50,000 tonnes of this material annually, making it a significant resource. XRD analysis of SA indicated its composition as 77% sodium sulfate (Na_2SO_4), 5% thenardite, and 17.6% nahcolite, as determined by Rietveld refinement. Furthermore, the alkalinity of a 5% SA solution was measured to be within a pH range of 7.5–8 according to ISO 6353/2:1983 standards. Ion chromatography and ICP-MS analyses revealed the metallic content in SA, with concentrations of 0.44% Na, 0.47% Al, 0.46% Cu, 0.32% Zn, 0.26% Mg, 0.16% Mn, 0.0021% As, and 0.001% Pb. These chemical and metallic characteristics make SA a potential candidate for integration into geopolymer systems as an alternative activator.

The mixture designs of the GCs in this experiment are shown in Table 2. A total of 6 groups of mixtures with different ratios were designed. The SS content was used at 40 wt% and the GGBFS content at 60 wt% in all mixes, maintaining a constant ratio across all designs. The amount of SA was used in the ratio SS+GGBFS at 5 wt%. The effect of the SP content was investigated using 5%, 10%, 15%, 15%, 20% and 25% by weight of GGBFS. For all GCs, the solution/powder (S/P) ratio was chosen to be 0.25 to ensure adequate workability and high compressive strength.

Table 2. Experimental design (g)

Codes	SS	GGBFS	SP	SA	NaOH (10M)	$Na_2SiO_{3(aq)}$
S0	40	60	0	5	5	20
S5	40	55	5	5	5	20
S10	40	50	10	5	5	20
S15	40	45	15	5	5	20
S20	40	40	20	5	5	20
S25	40	35	25	5	5	20

The steps involved in preparing GCs are illustrated in Figure 3. The triple activator solution (TAS) was created using NaOH, Na_2SiO_3(aq), sodium sulfate-based activator (SA), and tap water. The preparation process consisted of the following stages:

- Preparation of NaOH Solution: A 10 M sodium hydroxide solution was prepared by dissolving solid NaOH pellets in tap water. The solution was allowed to rest in a sealed glass container at room temperature for 24 hours to stabilize.
- Na_2SiO_3 Solution Preparation: A second solution was created by combining equal weights (50 wt%) of tap water due to its economy and workability and aqueous sodium silicate (Na_2SiO_3) in a glass beaker.
- Combining Solutions: For cost efficiency and ease of processing, the NaOH solution (20 wt%) and the water-Na_2SiO_3 solution (80 wt%) were blended using a magnetic stirrer. The combined solution served as the primary base for the TAS.
- Integration of SA: The sodium/silicate activator solution was then mixed with a constant proportion of SA using a hand mixer to ensure uniformity.

For the preparation of GCs, the specified amounts of SS, SP, and GGBFS for each group were weighed and initially combined in a JJ-5 mixing chamber. The materials were mixed at medium speed for 60 seconds to achieve a consistent blend. The preparation steps for the GCs involved two mixing phases:

- Phase 1: The TAS was added to the mixer, followed by the SS+SP+GGBFS mixture. These components were blended at a medium speed of 1400 rpm for 60 seconds.
- Phase 2: The mixture was further mixed at a higher speed of 2800 rpm for 300 seconds to ensure thorough homogenization.

This multi-step process was designed to optimize the quality and performance of the geopolymer composite mixtures.

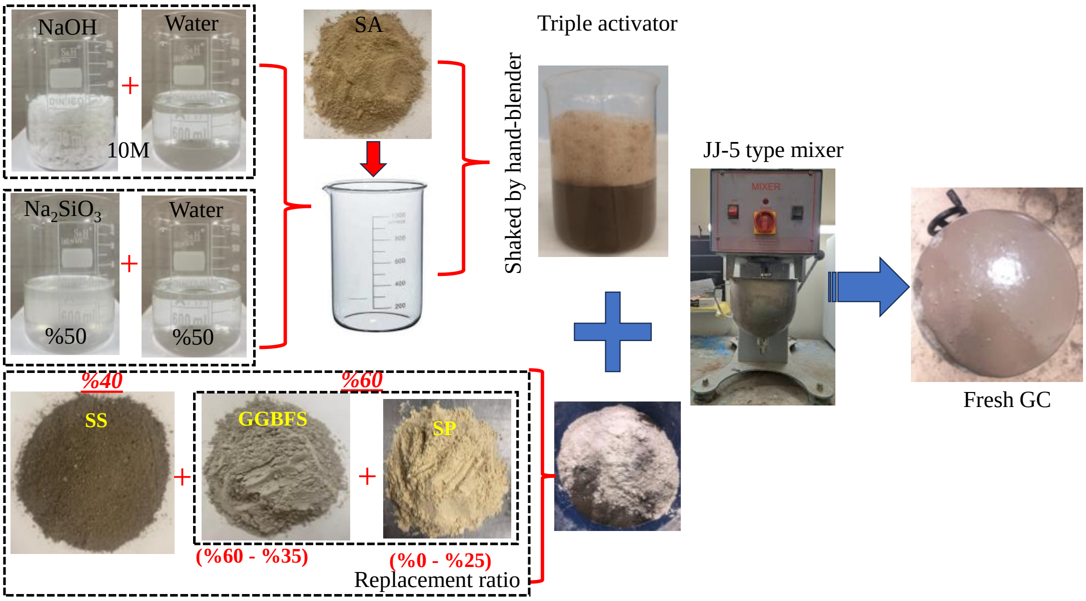

Figure 3. Manufacturing and preparation process of GCs

Following the guidelines of ASTM C1437-15 [31], the flowability of fresh GCs was determined using a material-loaded truncated cone mould. The mould was slightly raised, and the drop was activated 25 times. The workability of the GCs was assessed by recording the expansion diameter in two perpendicular directions and calculating the average. The GCs were then moulded into cubic shapes of 50x50x50 mm and cured under ambient laboratory conditions for 28 days in preparation for testing. The compressive strength test was carried out according to ASTM C109 [32] and the acid resistance test according to ASTM C267 [33] with GCs cast in 50x50x50 mm steel moulds. In order to perform the acid resistance test, a solution of 1% sulfuric acid was prepared by diluting concentrated sulfuric acid with distilled water. The specimens were stored under standard laboratory conditions for 28 days to provide sufficient curing time. Following the 28-day period, the specimens were immersed in the prepared sulfuric acid solution and left to soak for a further 30 days until the day of the experiment. The water absorption test was carried out according to ASTM C1585 [34]. The 40x40x160 mm specimens were subjected to shrinkage and capillary water absorption tests according to ASTM C596 - 18 [35] and ASTM C1585 [34]. The shrinkage measurements of the GCs were conducted at 1, 2, 3, 7, 14, 21, and 28 days. The measurements were taken using a micrometer on prisms measuring 40 x 40 x 160 mm at three points, and the mean of these three measurements was employed to calculate the shrinkage. The shrinkage was calculated using the following formula (1). The samples were cured in an oven at 80 °C for 2 hours before demoulding, as literature suggests that this condition yields the highest compressive strength [36-37] promoting early setting and improved early mechanical properties. All GCs were cured in the laboratory in ambient conditions (22±2 ºC, 30±5 R.H.) for 28 days until the testing days. The hardened GCs were tested for compressive strength and water absorption on days 2 and 28 to evaluate the evolution of the mechanical properties over time.

$$Shrinkage = \frac{Final\ Length - Initial\ Length}{Initial\ Length} \tag{1}$$

3. Results and Discussions

3.1. Workability of GCs

The results of the workability test of the GC mixtures are shown in Figure 4. As the SP ratio increased, the slump values of the GCs also increased. In particular, when the SP ratio was 10% or higher, the workability was improved due to the inert nature of SP compared to GGBFS and its lower specific surface area. When evaluating the spread values based on the S0-series, it was observed that when the SP ratio was 5% and ≥10%, the increase was approximately 23% and 46% respectively.

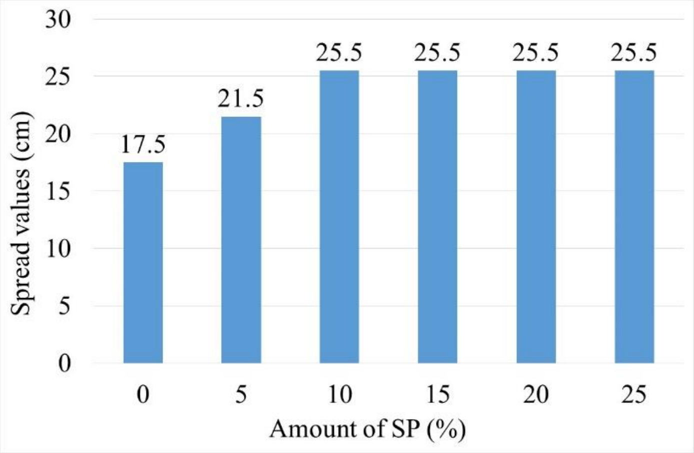

Figure 4. The results of the workability of GCs

3.2. Compressive strength of GCs

The compressive strength results of the GCs are shown in Figure 5. The highest compressive strengths at 2 and 28 days were 46.48 MPa and 74.31 MPa respectively for the S0 series. However, the S5 series had compressive strengths that were 7% lower than the S0 series. The lowest compressive strength at 2 and 28 days was achieved by the S5 series with values of 13.28 MPa and 34.59 MPa respectively. For the S5, S10, S15, S20 and S25 grades, the 2-day compressive strengths decreased by 6.7%, 14.6%, 35.7%, 185.5% and 250% respectively compared to S0, while at 28 days the decreases were 3.9%, 16.6%, 32.9%, 52.1% and 114.8% respectively. The reduction in the reactive GGBFS content and the increase in the inert SP ratio resulted in a reduction in compressive strength. The decrease in strength was caused by a decrease in the formation of C-A-S-H gels, which are responsible for the increase in strength. Replacement of SP at 5% by weight did not disturb the stoichiometric ratio, whereas replacement above 10% SP disturbed the stoichiometric ratio. The stoichiometric ratio refers to the optimal balance between the alkaline activator and the aluminosilicate source required for the geopolymerization reaction. Maintaining this ratio is crucial for ensuring the complete reaction of the precursor materials and achieving the desired mechanical properties in the ultimate GCs. At 28 days, the compressive strengths for the S0, S5, S10, S15, S20 and S25 series increased by approximately 60%, 60%, 57%, 63%, 200% and 161% respectively compared to the 2-day values. The increase in SP content over time enhances gel formation, as SiO_2 dissolves in the alkaline medium, which contributes to the improved compressive strength development, as reported in the literatüre [30].

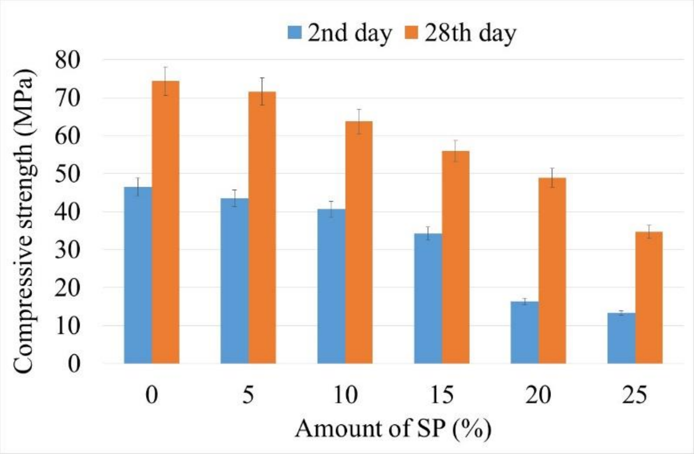

Figure 5. Results of the compressive strength of all GCs

3.3. Water absorption of GCs

The water absorption results for the GCs are shown in Figure 6. As the inert SP content increased, the reduction in reactive GGBFS resulted in a decrease in reactions, leading to an increase in visible porosity. In addition, the reduction in GGBFS resulted in a reduction in C-S-H, C(N)-A-S-H, gypsum or ettringite gel formation, which typically fills voids. Apparent porosity in the S5, S10, S15, S20 and S25 series increased by 4.8%, 12.63%, 18.19%, 29.59% and 33.08% respectively compared to the S0 series. Since the apparent porosity of the S5 series was 5% lower than that of the S0 series, its compressive strength was 7% lower. This aligns with the literatüre [38], which suggests that when apparent porosity is below 5%, its effect on compressive strength is minimal. As the amount of GGBFS, which has a higher specific gravity than SP, decreased, the dry bulk density also decreased. The lowest dry specific weight of 1.72 was found in the S5 range. There is a linear relationship between water absorption values and compressive strength.

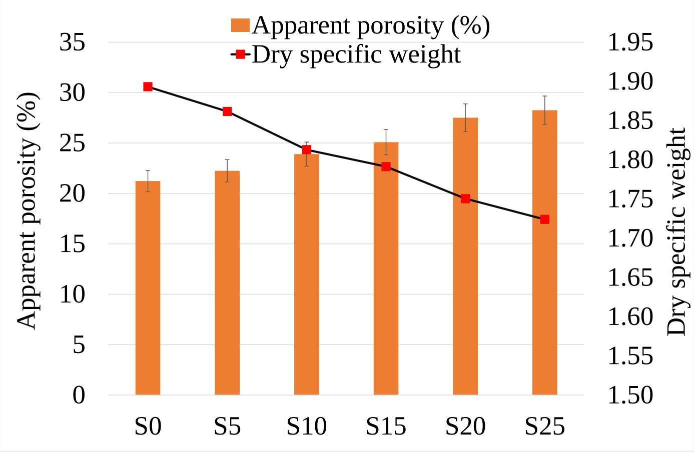

Figure 6. Results of apparent porosity and dry specific weight of GCs

3.4. Length change measurements of GCs

The results of the shrinkage test for the GCs are presented in Figure 7. The highest and lowest shrinkage values were observed in the S25 and S5 series, with values of 2.6% and 1.7%, respectively. The 5% replacement of SP interacts with the Ca^{2+} component present in sufficient quantities in the geopolymer composition, resulting in a reaction with SiO_2 that enhances gel formation. Consequently, the filling of micro and macro voids reduces shrinkage. Furthermore, an analysis of the apparent porosity and capillarity coefficient indicates that the voids in the S5 series were filled through gelation. As the shrinkage values increased, the compressive strength decreased, and the apparent porosity increased. A review of the literature reveals that reaction products in GCs can significantly fill voids, thereby influencing both shrinkage and absorption. For instance, Xie etc. report in their review article that the formation of reaction products contributes to a reduction in porosity and void spaces, which in turn influences the material's shrinkage and absorption properties [39]. Apart from the S5 series, the shrinkage values of the remaining geopolymer composites were higher than those of the S0 series. When the SP replacement ratio exceeded 10%, the shrinkage values increased due to the reduction in gel formation caused by chemical reactions.

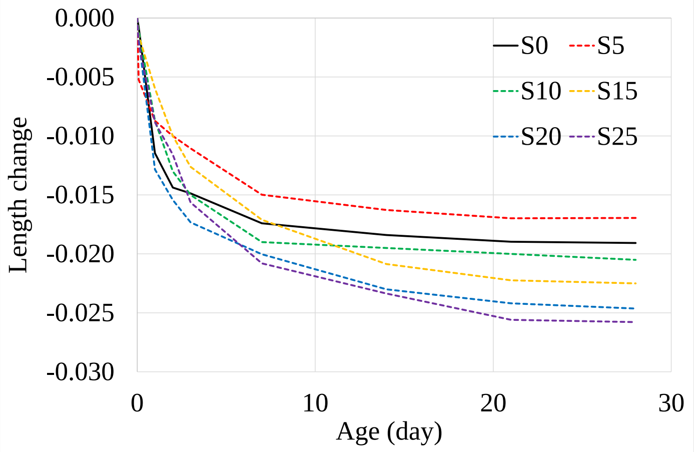

Figure 7. Shrinkage measurements of all GCs

3.5. Capillary water absorption of GCs

The results of the capillary water absorption test are presented in Figure 8. The lowest capillary coefficient, 0.89 (g/cm²√min), was observed in the S5 series. The replacement of 5% of the mixture with SP resulted in the dissolution and reaction of the silica with the Ca^{2+} components, which promoted gel formation and filled the capillary voids. Consequently, the capillary coefficient fell below 1. However, when the SP content exceeded 5%, the reduction in GGBFS content led to a decrease in Ca^{2+}, and the reduction in gel formation caused the capillary voids to remain unfilled, resulting in an increase in the capillary coefficient.

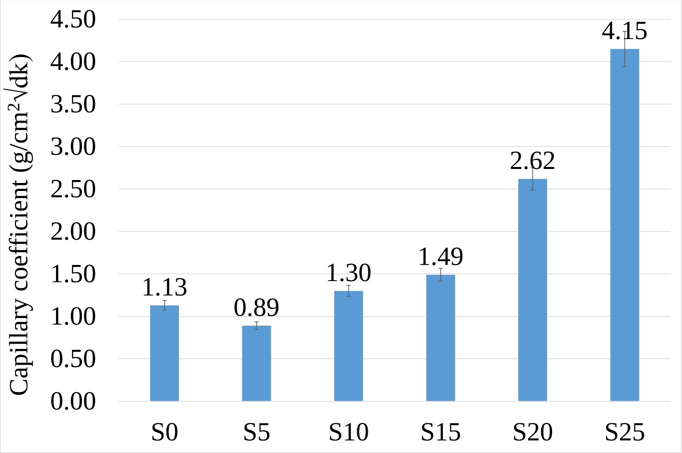

Figure 8. Results of capillary water absorption of GCs

The capillary water absorption test results presented in Figures 9a, b, and c are correlated with compressive strength, apparent porosity, and shrinkage values, with R^2 values of 0.93, 0.87, and 0.91, respectively. As the capillarity coefficient increased, the compressive strength decreased, the apparent porosity increased, and the shrinkage values also increased. These correlations indicate that higher capillary water absorption is linked to poorer mechanical properties and increased porosity, thereby highlighting the impact of capillary behaviour on the performance of GCs.

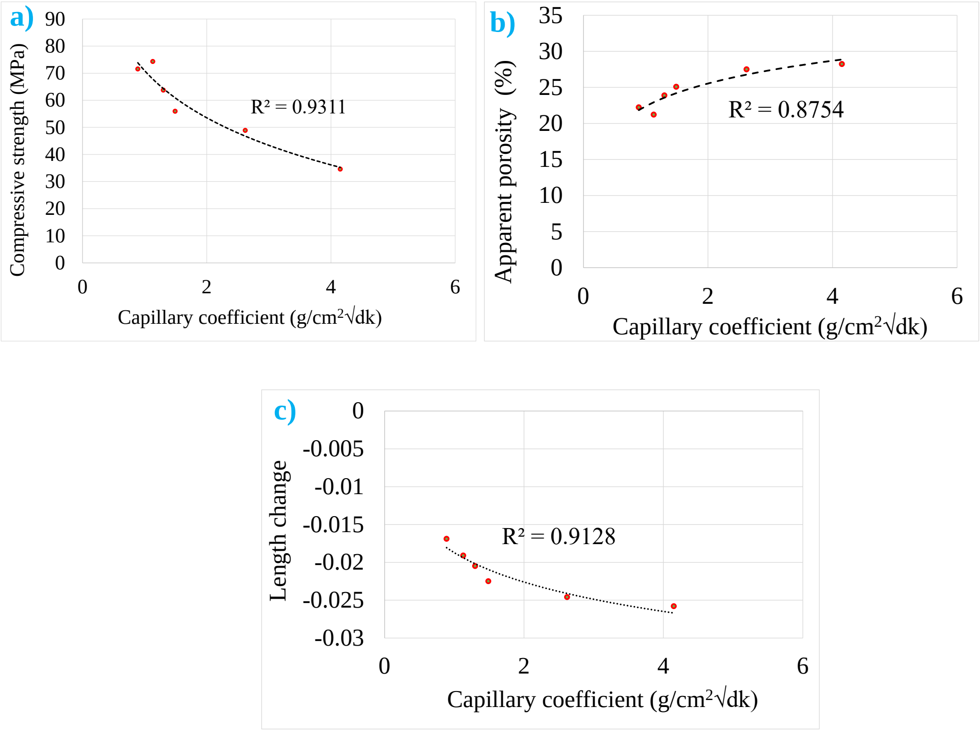

Figure 9. The capillary coefficient correlated with a) compressive strength, b) apparent porosity, and c) shrinkage values

3.6. Acid resistance of GCs

Figure 10a and b illustrate the acid resistance test results for GC specimens exposed to sulfuric acid for 30 days. The figures show mass loss and compressive strength loss, respectively. The geopolymers demonstrated volume stability and did not disintegrate after 30 days, indicating the formation of a geopolymer structure with robust characteristics, as shown in Figure 11. The lowest and highest mass losses, at 4.35% and 6.32%, respectively, were observed in the S0 and S25 series. As the SP content increased, a corresponding increase in mass loss was observed. In comparison to the S0 series, the mass loss for 5%, 10%, 15%, 20%, and 25% SP substitutions increased by 9.65%, 20.46%, 21.15%, 32.64%, and 45.29%, respectively. However, the mass losses observed in the S0 and S5 series remained below 5%. As illustrated in Figure 10b, the compressive strength exhibited a loss of 4.72%, 4.94%, and 5.56% for the S0, S5, and S10 series, respectively. The exposure of the material to sulfuric acid resulted in a reduction in pH, which led to the dissolution of C-S-H, ettringite, gypsum, and C(N)-A-S-H gels. This, in turn, led to a decrease in compressive strength. Nevertheless, the compressive strength losses in the S0, S5, and S10 series remained within the acceptable 5% limit. As the concentration of silica powder in the acidic medium increases, the amount of dissolved SiO_2 also increases in accordance with the solubility of the substance. The dissolution of SiO_2 enhances the formation of C(N)-A-S-H gels by reacting with free Ca^{2+} and Na^{2+} ions in the medium, thereby leading to an improvement in compressive strength in the S15, S20, and S25 series after sulfuric acid exposure.

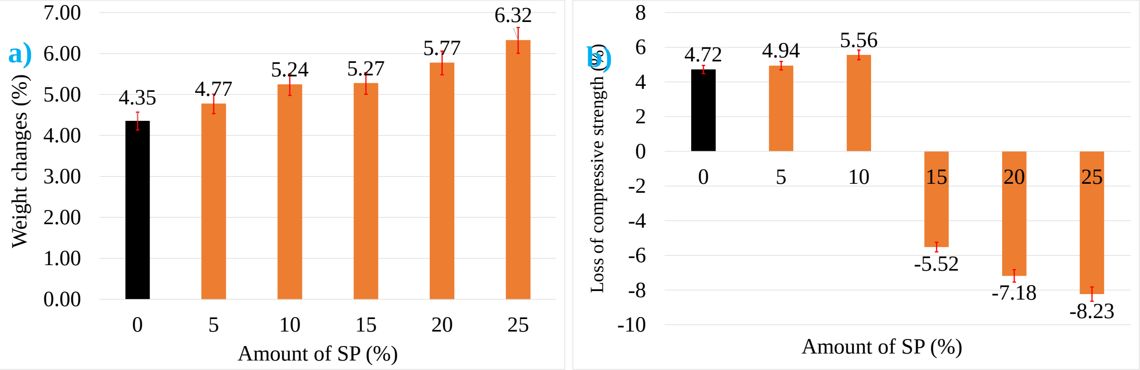

Figure 10. Acid resistance experiment results of GCs

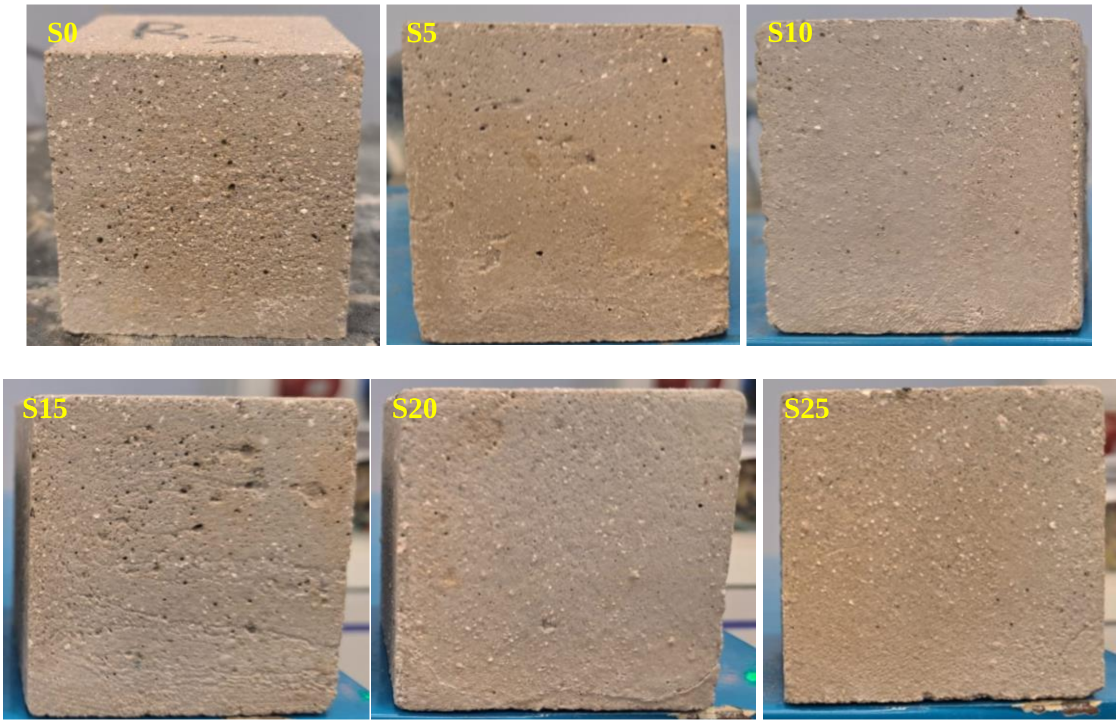

Figure 11. Images of GCs after 30 days of exposure to acid

4. Conclusıons

The primary objective of this study is to evaluate the fresh, hardened and durability properties of steel slag based geopolymer composites, with particular emphasis on the effect of silica powder (SP) as a partial precursor in combination with ternary activators such as NaOH, Na_2SiO_3(aq) and sintered ash. The findings of this study demonstrated that the most optimal ratio was 5% SP. An increase in the SP ratio enhances the workability of the GCs. The GCs employing 5% SP exhibited the closest approximation to the highest early and late strengths, with values of approximately 44 MPa and 72 MPa, respectively. Compared to the S0 series, the compressive strength of the S10, S15, and S20 series decreased by approximately 17%, 33%, and 52%, respectively, while the apparent porosity increased by approximately 13%, 18%, and 30%, respectively. The utilization of 5% SP decreased the apparent porosity and capillary water absorption values, indicating that it reduced the impermeability of the GCs. In acid medium, as the SP ratio increased, GCs mass loss increased, while compressive strength increased in the series with 15%, 20% and 25% substituted SP.

Acknowledgment

The authors would like to thank the Scientific Research Project of Turkey (BAP) for supporting this study by funding it as a part of the Karabük University, KBÜBAP-23-KP-058 project. The authors would like to thank Kardemir Steel Industry A.Ş. for providing the waste materials for this study.

Author Contribution

The authors confirm responsibility for the following: study conception and design, data collection, analysis and interpretation of results, and manuscript preparation.

Conflict of Interest

The authors declare that they have no conflict of interest.

References

[1] Mehta A, Ashish DK. Silica fume and waste glass in cement concrete production: A review. Journal of Building Engineering 2020; 29(5): 100888.
[2] Jiang Y, Ling TC, Mo KH, Shi C. A critical review of waste glass powder – Multiple roles of utilization in cement-based materials and construction products. Journal of Environmental Management 2019; 242: 440–449.
[3] Davidovits J. Geopolymers: Inorganic polymeric new materials. Journal of Thermal Analysis and Calorimetry 1989; 37(8): 1633–1656.
[4] Alnahhal MF, Kim T, Hajimohammadi A. Waste-derived activators for alkali-activated materials: A review. Cement and Concrete Composites 2021; 118(4): 103980.
[5] Abed FH, Zareei SA, Kurdi NH, Emami A. Enhancing geopolymer binder reactivity and performance via mechanochemical activation: A comprehensive study of rheological, mechanical, and microstructural properties. Construction and Building Materials 2024; 430(6): 136456.
[6] Provis JL, Duxson P, van Deventer JSJ. The role of particle technology in developing sustainable construction materials. Advanced Powder Technology 2010; 21(1): 2–7.
[7] Caldas PHCH, de Azevedo ARG, Marvila MT. Silica fume activated by NaOH and KOH in cement mortars: Rheological and mechanical study. Construction and Building Materials 2023; 400(10): 132623.
[8] Mohajerani A, Vajna J, Cheung THH, Kurmus H, Arulrajah A, Horpibulsuk S. Practical recycling applications of crushed waste glass in construction materials: A review. Construction and Building Materials 2017; 156: 443–467.
[9] Hamed YR, Elshikh MMY, Elshami AA, Matthana MHS, Youssf O. Mechanical properties of fly ash and silica fume based geopolymer concrete made with magnetized water activator. Construction and Building Materials 2024; 411(1): 134376.
[10] Li B, Gao A, Li Y, Xiao H, Chen N, Xia D, Wang S, Li C. Effect of silica fume content on the mechanical strengths, compressive stress–strain behavior and microstructures of geopolymeric recycled aggregate concrete. Construction and Building Materials 2023; 384(6): 131417.
[11] Tihomirovs P, De Maeijer PK, Korjakins A. Demolition waste glass usage in the construction industry. Infrastructures 2023; 8(12): 182.
[12] Azad NM, Samarakoon SMK. Utilization of industrial by-products/waste to manufacture geopolymer cement/concrete. Sustainability 2021; 13(2): 873.
[13] Zhang L, Wang Q, Zheng Y, Cang Z, Gisele K, Yu C, Cang D. Synergistic effect and mechanism of waste glass on the mechanical properties and autoclave stability of cementitious materials containing steel slag. Construction and Building Materials 2021; 311: 125295.

[14] Özsoy M, Fırat S. Numerical analysis of road infrastructure layers made with steel slag. Journal of Polytechnic 2023; 24(6): 1661-1673.
[15] Karadağ H, Fırat S, Işık NS. Utilization of steel slag as road base and subbase material. Journal of Polytechnic 2020; 23(3): 799-812.
[16] Uysal FF, Bahar S. Slag types and utilization areas. Trakya University Journal of Engineering Sciences 2018; 19(1): 37-52.
[17] Kua HW. Integrated policies to promote sustainable use of steel slag for construction—A consequential life cycle embodied energy and greenhouse gas emission perspective. Energy and Buildings 2015; 101: 133-143.
[18] Yi H, Xu G, Cheng H, Wang J, Wan Y, Chen H. An Overview of utilization of steel slag. Procedia Environmental Sciences 2012; 16: 791-801.
[19] Hasan MS, Najim K. Geopolymer concrete from steel slag: Mechanical and durability properties. Construction and Building Materials 2018; 190: 1152-1161.
[20] Zheng Z, Deng P. Mechanical and fracture properties of slag/steel slag-based geopolymer fully recycled aggregate concrete. Construction and Building Materials 2024; 413: 134533.
[21] Mansourghanaei MH, Biklaryan M, Mardookhpour A. Durability and mechanical properties of granulated blast furnace slag-based geopolymer concrete containing polyolefin fibers and nano silica. KSCE Journal of Civil Engineering 2024; 28: 209–219.
[22] Ayim-Mensah G, Radosavljevic M. Influence of ground granulated blast furnace slag on the compressive strength and ductility of ultra high-performance fibre reinforced cementitious composites. Cement 2022; 8(6): 100030.
[23] Peng MX, Wang ZH, Shen SH, Guo XQ, Jiang LL, Cheng YC, Lin HL. One-part geopolymeric cements cured at elevated temperature by comparison with two-part ones. Construction and Building Materials 2017; 130: 103-112.
[24] Yu S, He J, Sang G, Yang SQ, Liu G. Study on hydration process of alkali-activated slag cement activated by weakly alkaline components. Construction and Building Materials 2024; 413: 134716.
[25] Rashad AM, Bai Y, Basheer PAM, Milestone NB, Collier NC. Hydration and properties of sodium sulfate activated slag. Cement and Concrete Composites 2013; 37(1): 20-29.
[26] Li Y, Lei W, Zhang Q, Yang Q, He X, Su Y, Tan H, Liu J, Wang G. Synergistic effects of steel slag and wet grinding on ambient cured ground granulated blast furnace slag activated by sodium sulfate. Construction and Building Materials 2022; 349: 128661.
[27] Liu X, Li Y, Chen Z. Enhancing acid resistance of geopolymers through optimized raw material selection and curing conditions. Journal of Sustainable Materials 2024; 15(2): 227-237.
[28] Mohamed OA, Al-Khattab R, Al-Hawat W. Resistance to acid degradation, sorptivity, and setting time of geopolymer mortars. Front Struct Civ Eng 2022; 16: 781–791.
[29] Zhang B, Zhu H, Feng P, Zhang P. A review on shrinkage-reducing methods and mechanisms of alkali-activated/geopolymer systems: Effects of chemical additives. Journal of Building Engineering 2022; 49: 104056.
[30] Smith A, Johnson B, Lee C. Effect of NaOH concentration on the mechanical and physical properties of geopolymers. Journal of Materials Science 2023; 58(12): 3245-3258.
[31] ASTM C1437-15, Standard Test Method for Flow of Hydraulic Cement Mortar, PA, USA, 2015.
[32] ASTM C109-16, Standard Test Method for Compressive Strength of Hydraulic Cement Mortars, American Society for Testing and Materials, ASTM, PA, USA, 2016.
[33] ASTM C267-17, Standard Test Methods for Chemical Resistance of Mortars, Grouts, and Monolithic Surfacings, American Society for Testing and Materials, ASTM, PA, USA, 2017.
[34] ASTM C1585-13, Standard Test Method for Measurement of Rate of Absorption of Water by Hydraulic-Cement Concretes, American Society for Testing and Materials, ASTM, PA, USA, 2013.
[35] ASTM C596-18, Standard Test Method for Drying Shrinkage of Mortar Containing Hydraulic Cement, American Society for Testing and Materials, ASTM, PA, USA, 2018.
[36] Pekgöz M, Tekin İ. The Effects of different origins naoh on the mechanical and microstructural properties of tuff-based alkali-activated pastes. Turkish Journal of Engineering Research and Education 2022; 1(1): 29-37. doi: 31.05.2022.

[37] Tekin İ, Gencel O, Gholampour A, Oren OH, Koksal F. Recycling zeolitic tuff and marble waste in the production of eco-friendly geopolymer concretes. Journal of Cleaner Production 2020; 246: 119039.
[38] Zhang X, Li Y, Wang Z. A Study on relationship between porosity and compressive strength for geopolymer paste. Journal of Materials Science 2023; 58(4): 1123-1135.
[39] Xie W, Zhang M, Li S. A review on the effects of reaction products on the properties of geopolymer materials. Construction and Building Materials 2023; 345: 129558.